SLAC-PUB-2140
June 1978

INTRODUCTION TO INTENSITY INTERFEROMETRY FOR NUCLEAR-PARTICLE PHYSICISTS*

Alan Katz
Stanford Linear Accelerator Center
Stanford University, Stanford, California 94305

ABSTRACT

The Hanbury-Brown and Twiss method for measuring the radii of stars also has interesting applications in other realms of physics. Intensity interferometry, the technique used by Hanbury-Brown and Twiss for their star measurements, should yield analogous information about the angular sizes of excited particles and nuclei, which emit secondary particles. In this report, we interpret such emissions and the correlation functions that arise from considering registration probabilities at two space or time points in terms of the language of optics and diffraction theory. Our objective is to review the physics involved in the Hanbury-Brown and Twiss effect and to point out possible applications to problems in nuclear and particle physics.

(Submitted for Publication)

*Work supported by the Department of Energy.

I. RADIO TRANSMITTERS

As an introduction to interference phenomena and correlation functions, it is useful to consider the following experiment (see Fig. 1). Two radio transmitters are located at points (1) and (2) and emit spherical wave forms, which are detected at points (3) and (4). Points (3) and (4) are points of a circular arc, centered at C. Assuming that the transmitters emit independently, we can write the wave amplitudes at points (3) and (4) as follows:

$$A_3 = \left[\frac{S_1}{r_{13}} \exp\, i\left(\bar{K}r_{13} + \phi_1(t-r_{13/v})\right) + \frac{S_2}{r_{23}} \exp\, i\left(\bar{K}r_{24} + \phi_2(t-r_{24/v})\right)\right] \exp{-i\bar{w}t}$$

$$A_4 = \left[\frac{S_1}{r_{14}} \exp\, i\left(\bar{K}r_{14} + \phi_1(t-r_{14/v})\right) + \frac{S_2}{r_{24}} \exp\, i\left(\bar{K}r_{24} + \phi_2(t-r_{24/v})\right)\right] \exp{-i\bar{w}t}$$

where

$$r_{13} = |\vec{R}-\vec{r}_1| \qquad r_{23} = |\vec{R}-\vec{r}_2|$$

$$r_{14} = |\vec{R}'-\vec{r}_1| \qquad r_{24} = |\vec{R}'-\vec{r}_2|$$

and v is the velocity of the outgoing wave.

Remarks

1. We have assumed that both detectors emit wave packets strongly peaked about the wave number, $\bar{K}$.

2. The functions ϕ_1 and ϕ_2 are, in general, time dependent (real) functions which set the phases of the transmitters.

3. For convenience, we will assume $S_1=S_2$ and that these amplitudes are time independent.

In most situations of interest, $|\vec{R}| >> |\vec{r}_1|,|\vec{r}_2|$.

Using this inequality, we can write:

$$|\vec{R}-\vec{r}_i| = \left[(\vec{R}-\vec{r}_i)\cdot(\vec{R}-\vec{r}_i)\right]^{\frac{1}{2}} = (R^2 + r_i^2 - 2\vec{R}\cdot\vec{r}_i)^{\frac{1}{2}}$$

$$= R\left(1+(r_{i/R})^2 - \frac{2\hat{R}\cdot\vec{r}_i}{R}\right)$$

$$\approx R\left(1 - \frac{\hat{R}\cdot\vec{r}_i}{R}\right) = R-\hat{R}\cdot\vec{r}_i$$

Second-order terms in $(r_{i}/_{R})$ have been ignored.

Similarly, $|\vec{R}'-\vec{r}_i| \approx (R-\hat{R}'\cdot\vec{r}_i)$.

Hence, we can estimate A_3 and A_4 as follows:

$$A_3 = \frac{S_1}{R} \exp-i\bar{w}t \left[\exp i\left[\bar{K}(R-\hat{R}\cdot\vec{r}_1) + \phi_1\left(t - \frac{R-\hat{R}\cdot\vec{r}_1}{v}\right)\right]\right.$$
$$\left. + \exp\left[i\ \bar{K}(R-\hat{R}\cdot\vec{r}_2) + \phi_2\left(t - \frac{R-\hat{R}\cdot\vec{r}_2}{v}\right)\right]\right]$$

$$A_4 = \frac{S_1}{R} \exp-i\bar{w}t \left[\exp i\left[\bar{K}(R-\hat{R}'\cdot\vec{r}_1) + \phi_1\left(t- \frac{R-\hat{R}'\cdot\vec{r}_1}{v}\right)\right]\right.$$
$$\left. + \exp i\left[\bar{K}(R-\hat{R}'\cdot\vec{r}_2) + \phi_2\left(t- \frac{R-\hat{R}'\cdot\vec{r}_2}{v}\right)\right]\right]$$

In classical electromagnetic theory, we might think of A_3 and A_4 as components of the electric or magnetic field. The intensity of the electromagnetic disturbance at points (3) and (4), then, is respectively:

$$I_3 \alpha |A_3|^2 = \frac{|S_1|^2}{R^2}\Big[2 + \exp\, i\big[\bar{K}(\hat{R}\cdot\vec{r}_2 - \hat{R}\cdot\vec{r}_1) + (\phi_2 - \phi_1)\big]$$

$$+ \exp\, -i\big[\bar{K}(\hat{R}\cdot(\vec{r}_2 - \vec{r}_1) + (\phi_2 - \phi_1)\big]\Big]$$

$$= \frac{2|S_1|^2}{R^2}\Big[1 + \cos\Big[\bar{K}\hat{R}\cdot(\vec{r}_2 - \vec{r}_1) + \phi_2\Big(t - \frac{R - \hat{R}\cdot\vec{r}_2}{v}\Big)$$

$$-\phi_1\Big(t - \frac{R - \vec{R}\cdot\vec{r}_1}{v}\Big)\Big]\Big]$$

$$I_4 \propto |A_4|^2 = \frac{2|S_1|^2}{R^2}\Big[1 + \cos\Big[\bar{K}\hat{R}'\cdot(\vec{r}_2 - \vec{r}_1) + \phi_2\Big(t - \frac{R - \hat{R}'\cdot\vec{r}_2}{v}\Big)$$

$$-\phi_1\Big(t - \frac{R - \hat{R}'\cdot\vec{r}_1}{v}\Big)\Big]\Big]$$

For fixed phase functions (ϕ_1 and ϕ_2 independent of time), the conditions on the argument of the cosine functions that define the intensity maxima and minima are easily found. However, if ϕ_1 and ϕ_2 are random functions of time (such that the phase jumps around a lot in the time interval necessary to make the measurement), then it is necessary to average I_3 and I_4 over a time interval long compared to the interval between an average jump. In this case, I_3 and I_4 reduce to (constant) $\times\ 2|S_1|^2/R^2$, and it is seen that all spatial dependence is lost.

However, a harmonic spatial dependence results when the product of I_3 and I_4 is taken prior to performing the average, provided that points (3) and (4) are within a "coherence" length of each other:

$$I_3I_4 \propto |A_3|^2|A_4|^2 = \frac{4|S_1|^4}{R^4}(1 + \cos[b] + \cos[a] + \cos[a]\cos[b])$$

where

$$[a] = \left[\bar{K}\hat{R}'\cdot(\vec{r}_2-\vec{r}_1) + \phi_2\left(t-\frac{R-\hat{R}'\cdot\vec{r}_2}{v}\right)-\phi_1\left(t-\frac{R-\hat{R}'\cdot\vec{r}_1}{v}\right)\right]$$

$$[b] + \left[\bar{K}\hat{R}\cdot(\bar{r}_2-\vec{r}_1)+\phi_2\left(t-\frac{R-\hat{R}\cdot\vec{r}_2}{v}\right)-\phi_1\left(t-\frac{R-\hat{R}\cdot\vec{r}_1}{v}\right)\right]$$

Making use of the trigonometric identity

$$\cos a \cos b = \tfrac{1}{2}\cos(a-b) + \tfrac{1}{2}\cos(a+b) \quad ,$$

we find:

$$I_3I_4 = \frac{4|S_1|^4}{R^4}\left[\cos[b] + \cos[a]+1+\tfrac{1}{2}\cos([a]-[b])+\tfrac{1}{2}\cos([a]+[b])\right]$$

$$= \frac{4|S_1|^4}{R^4}\Bigg[1 + \cos[b] + \cos[a]+\tfrac{1}{2}\cos\Bigg\{\bar{K}(\hat{R}'-\hat{R})\cdot(\vec{r}_2-\vec{r}_1)+\phi_2\left(t-\frac{R-\hat{R}'\cdot\vec{r}_2}{v}\right)$$

$$-\phi_2\left(t-\frac{R-\hat{R}\cdot\vec{r}_2}{v}\right)+\phi_1\left(t-\frac{R-\hat{R}\cdot\vec{r}_1}{v}\right)-\phi_1\left(t-\frac{R-\hat{R}'\cdot\vec{r}_1}{v}\right)\Bigg\} +\tfrac{1}{2}\cos(\cdot[a]+[b])\Bigg] \quad .$$

Now, if the detectors are sufficiently close such that $(\hat{R}'-\hat{R})\cdot\vec{r}_2$ and $(\hat{R}'-\hat{R})\cdot\vec{r}_1$ are small compared to the coherence length (the distance over which interference phenomena are appreciable or, for this example, (v × the average time between phase jumps $\cong \ell_{coherent}$)), then

$$\left[\phi_2\left(t-\frac{R-\hat{R}'\cdot\vec{r}_2}{v}\right)-\phi_2\left(t-\frac{R-\hat{R}\cdot\vec{r}_2}{v}\right)\right] \cong$$

$$\left[\phi_1\left(t-\frac{R-\hat{R}\cdot\vec{r}_1}{v}\right)-\phi_1\left(t-\frac{R-\hat{R}'\cdot\vec{r}_1}{v}\right)\right] \cong 0$$

Thus

$$\langle I_3I_4\rangle^{\dagger} = \frac{4|S_1|^4}{R^4}\left[1+\tfrac{1}{2}\cos\{\bar{K}(\hat{R}-\hat{R}')\cdot(\vec{r}_2-\vec{r}_1)\}\right]$$

It may be concluded that even if the average intensity shows no variation over the circle, the product of the intensities at two points sufficiently near each other will still display a harmonic variation (in spatial coordinates). For this reason, $\langle I_3 I_4 \rangle$ is called a correlation function. An explanation for such a correlation is not hard to come by; it is a reflection of the fact that any phase change that affects the wave amplitude at a given point on the circle will simultaneously affect the amplitudes at all points within a coherence length of the given point. This implies that the degree of correlation between points (3) and (4) is preserved: For example, if a maximum at (3) implies a maximum at (4), then a minimum at (3) implies a minimum at (4).

The circular arrangement of detectors that we have been discussing is special in the sense that for $|\vec{r}_2|, |\vec{r}_1| << \ell_{\text{COHERENCE}}$ $\langle I_3 I_4 \rangle$ is spatially dependent for every pair of points on the circle. For our example, then, we need not be too concerned with coherence length and times as long as the above condition on $|\vec{r}_2|$ and $|\vec{r}_1|$ is met.

II. TIME CORRELATIONS

Time correlations are a natural extension of what has been done so far. The precise meaning of a time correlation (as opposed to the spatial correlation considered above) is made evident by examining once more our experiment with two radio transmitters. Now, however, the transmitters will be emitting at different frequencies, $\bar{w}_1$ and $\bar{w}_2$. Moreover, the two detectors will be placed at the same spatial point. The correlation function that will be of interest is of the form $I_3(t) I_3(t + \tau)$, where $I_3(t)$ is the intensity reading at point (3), at time t, and $I_3(t+\tau)$ is the intensity reading at the same point but at the delayed time, $t+\tau$.

$$A_3(t) = \frac{S_1}{R}\left[\exp\ i\left(\bar{K}_1 r_{13}+\phi_1\left(t-\frac{r_{13}}{v}\right)-\bar{w}_1 t\right)+\exp\ i\left(\bar{K}_2 r_{23}+\phi_2\left(t-\frac{r_{23}}{v}\right)-\bar{w}_2 t\right)\right]$$

$$A_3(t+\tau) = \frac{S_1}{R}\left[\exp\ i\left(\bar{K}_1 r_{13}+\phi_1\left(t+\tau-\frac{r_{13}}{v}\right)-\bar{w}_1(t+\tau)\right)\right.$$

$$\left.+\exp\ i\left(\bar{K}_2 r_{23}+\phi_2\left(t+\tau-\frac{r_{23}}{v}\right)-\bar{w}_2(t+\tau\right)\right)\right]$$

The intensities at the two time points are proportional to:

$$|A_3(t)|^2 = \frac{|S_1|^2}{R^2}\left[2+\exp\ i\left(\bar{K}_1 r_{13}-\bar{K}_2 r_{23}+\phi_1\left(t-\frac{r_{13}}{v}\right)-\phi_2\left(t-\frac{r_{23}}{v}\right)+(\bar{w}_2-\bar{w}_1)t\right)\right.$$

$$\left.+\exp-i\left(\bar{K}_1 r_{13}-\bar{K}_2 r_{23}+\phi_1\left(t-\frac{r_{13}}{v}\right)-\phi_2\left(t-\frac{r_{23}}{v}\right)+(\bar{w}_2-\bar{w}_1)t\right)\right]$$

$$= \frac{2|S_1|^2}{R^2}\left[1+\cos\left\{\bar{K}_1 r_{13}-\bar{K}_2 r_{23}+\phi_1\left(t-\frac{r_{13}}{v}\right)-\phi_2\left(t-\frac{r_{23}}{v}\right)+(\bar{w}_2-\bar{w}_1)t\right\}\right]$$

and

$$|A_3(t+\tau)|^2 = \frac{2|S_1|^2}{R^2}\left[1+\cos\left\{\bar{K}_1 r_{13}-\bar{K}_2 r_{23}+\phi_1\left(t+\tau-\frac{r_{13}}{v}\right)\right.\right.$$

$$\left.\left.-\phi_2\left(t+\tau-\frac{r_{23}}{v}\right)+(\bar{w}_2-\bar{w}_1)(t+\tau)\right\}\right]$$

Hence, the time average of the product of intensities is given, to within a proportionality factor, by:

$$\langle I_3(t)I_3(t+\tau)\rangle \propto \frac{4|S_1|^4}{R^4}\left[1+\tfrac{1}{2}\left\langle\cos\left(\phi_1\left(t+\tau-\frac{r_{13}}{v}\right)\right.\right.\right.$$

$$-\phi_1\left(t-\frac{r_{13}}{v}\right)+\phi_2\left(t-\frac{r_{23}}{v}\right)$$

$$\left.\left.\left.-\phi_2\left(t+\tau-\frac{r_{23}}{v}\right)+(\bar{w}_2-\bar{w}_1)\tau\right)\right\rangle\right]$$

Now, for $\tau < t_C$ (the coherence time), we have:

$$\langle I_3(t)I_3(t+\tau)\rangle \propto \frac{4|S_1|^4}{R^4}\left[1+\tfrac{1}{2}\cos(\bar{w}_2-\bar{w}_1)\tau\right]$$

Hence, there is a harmonic variation in τ only if $\tau < t_C$ and $\bar{w}_2 \neq \bar{w}_1$. Applications of the concept of time correlation and further discussion of coherence time, as related to the spectral width, can be found in Born and Wolf, Principles of Optics, 5th Ed., § 10.7.3.

III. CONTINUOUS, ALMOST MONOCHROMATIC SOURCE

We now take up the more complicated problem of determining the correlation function for two points on a screen illuminated by a continuous monochromatic source.[1] This problem serves both to expand the notion of the correlation function and to provide a connection between the correlation function and diffraction theory (via the Van Cittert-Zernike Theorem). This connection will prove useful when we discuss the emission of particles from an excited nucleus.

The extended source (x',y')--see Fig. 2--is taken to be parallel to the plane, (x,y). Moreover, the overall dimensions of the source are assumed to be small compared to the distance R. For the purpose of calculating the total disturbance at a point, P, it is useful to divide (x',y') into sections small compared to the wavelength of the disturbance and, then, to sum the contributions from each of these sections. For a countable number of sections, the total disturbances registered at points P_1 and P_2 are

$$V_1(t) = \sum_m V_{1m}(t) \quad , \quad V_2(t) = \sum_m V_{2m}(t)$$

respectively.

Making use of the fact that

$$\left\langle V_1^{(REAL)}(t)\ V_2^{(REAL)}(t)\right\rangle$$

is proportional to $\langle V_1(t)V_2^*(t)\rangle$, and that $V_1(t)$ and $V_2(t)$ are complex,[2] we define the following correlation function:

$$J(P_1,P_2) = \langle V_1(t)V_2^*(t)\rangle = \left\langle \sum_m V_{m1}(t) \sum_m V_{m2}^*(t)\right\rangle$$

$$= \sum_{m,n} \langle V_{m1}(t)V_{n2}^*(t)\rangle$$

$$= \sum_m \langle V_{m1}(t)V_{m2}^*(t)\rangle + \sum_m \sum_{\substack{n \\ m\neq n}} \langle V_{m1}(t)V_{n2}^*(t)\rangle$$

Now, for $m \neq n$, we can write

$$\langle V_{m1}(t)V_{n2}^*(t)\rangle = \langle V_{m1}(t)\rangle\langle V_{n2}^*(t)\rangle = 0$$

The first equality follows from the statistical independence of the sources whereas the second equality can be confirmed by allowing the functions $V_{m1}(t)$ or $V_{n2}(t)$ to have the functional form:

$$V_{m1}(t) = \frac{\sigma_{m1}}{r} \exp i\left(\Phi_{m1}\left(t-\frac{r}{v}\right)\right) \exp i(\bar{K}r-\bar{w}t)$$

(This form of $V_{m1}(t)$ is derived under the assumption that the wave packet is very strongly peaked about the wavenumber $\bar{K}$). Hence,

$$\langle V_{m1}(t)V_{n2}^*(t)\rangle = \frac{\sigma_{m1}}{r_{m1}}\frac{\sigma_{n2}^*}{r_{n2}} \langle \exp\ i\Phi_{m1}(t)\rangle\langle \exp -i\Phi_{m2}(t)\rangle$$

$$= 0\ .$$

This result allows us to write:

$$J(P_1,P_2) = \sum_m \langle V_{m1}(t)V^*_{m2}(t)\rangle$$

$$= \sum_m \frac{\sigma_m\sigma^*_m}{r_{m1}r_{m2}} \left\langle \exp i\left(\Phi_m\left(t-\frac{r_{m1}}{v}\right)-\Phi_m\left(t-\frac{r_{m2}}{v}\right)\right)\right\rangle \exp i\bar{K}(r_{m1}-r_{m2})$$

which becomes, after a change of variables

$$J(P_1,P_2) = \sum_m \frac{\sigma_m\sigma^*_m}{r_{m1}r_{m2}} \left\langle \exp i\left(\Phi_m(t)-\Phi_m\left(t+\frac{r_{m1}-r_{m2}}{v}\right)\right)\right\rangle \exp i\bar{K}(r_{m1}-r_{m2})$$

Now, if r_1-r_2 is small compared to the coherence length (the concept introduced in Section I), then

$$J(P_1,P_2) = \sum_m \frac{\sigma_m\sigma^*_m}{r_{m1}r_{m2}} \exp i\bar{K}(r_{m1}-r_{m2}) .$$

Since $\sigma_m\sigma^*_m$ characterizes the intensity of the source, in the continuum limit, we may write:

$$J(P_1,P_2) = \int I(S)\,\frac{\exp i\bar{K}(r_1-r_2)}{r_1r_2}\,dS ,$$

where I(S) is the intensity per unit area of the source. For a source of uniform intensity:

$$J(P_1,P_2) = I\int \frac{\exp i\bar{K}(r_1-r_2)}{r_1r_2}\,dS$$

The integral in the above expression corresponds to the Huygen-Fresnel result in scalar diffraction theory. This correspondence is expressed formally by the Van Cittert-Zernike theorem (which is found in Born and Wolf, Principles of Optics, 5th Edition, § 10.4). The theorem, however, as stated in Born and Wolf, applies to the complex degree of coherence, $\mu(P_1,P_2)$, defined as

$$\mu(P_1,P_2) = \frac{J(P_1,P_2)}{\left(J(P_1,P_1)J(P_2,P_2)\right)^{\frac{1}{2}}}$$

Born and Wolf go on to show that

$$\mu(P_1,P_2) = \frac{(\exp i\Psi)\iint I(x',y')\exp -i\bar{K}(px'+qy')dx'dy'}{\iint I(x',y')dx'dy'}$$

where (x',y') are the coordinates of a typical source point, S; (X_1,Y_1) and (X_2,Y_2) are the coordinates of P_1 and P_2; and p, q, and Ψ are defined as follows:

$$\frac{(X_1-X_2)}{R} = p \qquad \frac{(Y_1-Y_2)}{R} = q$$

$$\Psi = \frac{\bar{K}}{2R}\left[(X_1^2+Y_1^2)-(X_2^2+Y_2^2)\right]$$

For the particular example of a uniform circular source of radius, a, Born and Wolf[3] compute:

$$\mu(P_1,P_2) = \left(\frac{2J_1(v)}{v}\right) \exp i\Psi$$

where

$$v = \frac{a\bar{K}}{R}\left((X_1-X_2)^2+(Y_1-Y_2)^2\right)^{\frac{1}{2}} .$$

IV. APPLICATION TO NUCLEI

The approach of Hanbury-Brown and Twiss to the measurement of stellar radii (which involves the computation of a correlation function related to $\langle I_3 I_4 \rangle$) is applicable to the emission of particles from an excited nucleus[4]; in place of a star, we deal with an excited nucleus that emits neutrons or pions. It is necessary, however, to distinguish the pion problem from the neutron one in terms of the statistics the particles obey. Pions are spin 0 particles and must be described by overall symmetric wave functions whereas neutrons are spin ½ and have antisymmetric wave functions. The consequences of this distinction will be discussed below.

As a first attempt at understanding the nuclear problem, we will consider the nucleus to have been excited since the beginning of time (t=0) and to be kept excited by a continual input of energy. In a proper treatment, the nucleus is excited at a particular time and decays exponentially.

Suppose now that we examine the particle emissions from the point of view of Section I. Two points on the nuclear surface may be regarded as independent emitters;[5] that is, if we consider a large ensemble of similarly excited nuclei, then any two points on the nuclear surface will be completely uncorrelated after averaging over the ensemble. Next, we set up two detectors and ask what the probability is for registering one particle in each detector at a time, t. The two surface elements lie sufficiently close to each other that it is impossible to decide from which source a particular particle came: The wave functions of the two emitted particles overlap. The means by which this ambiguity is incorporated into the formal description of the system is to treat the outgoing particles as identical bosons or fermions and, accordingly, to symmetrize or antisymmetrize the wave function.

When pions are simultaneously detected, the wave function is given by (see Fig. 3):

$$A_\pi = \frac{\exp\, i(p_3 r_{13} - E_3 t)/\hbar}{r_{13}} \frac{\exp\, i(p_4 r_{24} - E_4 t)/\hbar}{r_{24}}$$

$$+ \frac{\exp\, i(p_4 r_{14} - E_4 t)/\hbar}{r_{14}} \frac{\exp\, i(p_3 r_{23} - E_3 t)/\hbar}{r_{23}}$$

It should be noted that the detectors record the energies of the particles.

There is no need to worry about the spin part of the wave function since pions are spinless particles. Under particle exchange, which is effected most easily by switching the "1" and "2" indices, the amplitude A_π is seen to be symmetric.

The probability for detecting two pions simultaneously is given by:

$$|A_\pi|^2 = \frac{2}{R^4}\left[1+\cos\left(p_3(r_{13}-r_{23})+p_4(r_{24}-r_{14})\right)\right]$$

with

$$|\vec{r}_{1i}|,\ |\vec{r}_{2i}| \approx R$$

Next, we assume that the particles received by the detectors are spin ½ nucleons. In this case, there is a spin component of the wave function as well as a spatial part to consider. Assuming that the polarization of the nucleons is not fixed, we must give equal weight to the six possible antisymmetric wave functions for a two-state system:

$$(1)\quad A_N^1 = \underbrace{\frac{1}{\sqrt{2}}(|a\rangle|b\rangle-|b\rangle|a\rangle)}_{\text{space}}\ \underbrace{|\uparrow\uparrow\rangle}_{\text{spin}}$$

$$(2)\quad A_N^2 = \frac{1}{\sqrt{2}}(|a\rangle|b\rangle-|b\rangle|a\rangle)\,|\downarrow\downarrow\rangle$$

$$(3)\quad A_N^3 = \frac{1}{\sqrt{2}}(|a\rangle|b\rangle-|b\rangle|a\rangle)\,\frac{1}{\sqrt{2}}(|\uparrow\downarrow\rangle+|\downarrow\uparrow\rangle)$$

$$(4)\quad A_N^4 = \frac{1}{\sqrt{2}}(|a\rangle|b\rangle+|b\rangle|a\rangle)\,\frac{1}{\sqrt{2}}(|\uparrow\downarrow\rangle-|\downarrow\uparrow\rangle)$$

$$(5)\quad A_N^5 = |a\rangle|a\rangle\,\frac{1}{\sqrt{2}}(|\uparrow\downarrow\rangle-|\downarrow\uparrow\rangle)$$

$$(6)\quad A_N^6 = |b\rangle|b\rangle\,\frac{1}{\sqrt{2}}(|\uparrow\downarrow\rangle-|\downarrow\uparrow\rangle)$$

However, states (5) and (6) are not consistent with the bounds set by the experimental conditions. To see this, observe that if state $|a\rangle$ corresponds to a particle being at detector 3 and state $|b\rangle$ to a particle being at detector 4, then amplitudes (5) and (6) in the list above are the amplitudes for <u>both</u> particles being at a single detector. But the experiment we are discussing is blind to this possibility. The total probability for the simultaneous registration of two nucleons at detectors 3 and 4 involves only the first four amplitudes:

$$P_{spin\frac{1}{2}}(3,4) = |A_N^{1S}|^2+|A_N^{2S}|^2+|A_N^{3S}|^2+|A_N^{4S}|^2$$

$$\propto \frac{1}{R^4}\left(1-\tfrac{1}{2}\cos\left[p_3(r_{13}-r_{23})+p_4(r_{24}-r_{14})\right]\right)$$

where s=spatial part signifies the part of the wave function dependent on the spatial variable: for example, $A_N^{1S}=\frac{1}{\sqrt{2}}(|a\rangle|b\rangle-|b\rangle|a\rangle)$.

$$\cong\left(\frac{\exp\ i(p_3r_{13}-E_3t)/\hbar}{R}\right)\left(\frac{\exp\ i(p_4r_{24}-E_4t)/\hbar}{R}\right)$$

$$-\left(\frac{\exp\ i(p_4r_{14}-E_4t)/\hbar}{R}\right)\left(\frac{\exp\ i(p_3r_{23}-E_3t)/\hbar}{R}\right)$$

The reason for neglecting the spin part of the wave function in the above computation of $P_{spin\frac{1}{2}}$ stems from the orthonormality of the spin states. The absolute square of the wave function separates into the product of the space part times its complex conjugate <u>and</u> the inner product of the spin state with itself, which is 1(e.g. $\langle\uparrow\uparrow|\uparrow\uparrow\rangle$).

V. APPLICATION TO NUCLEI: CONTINUOUS SOURCE

So far, we have dealt only with a source composed of two independent emitters. The next step is to calculate the registration probability for an extended source. A useful example is the uniformly radiating sphere.

Before turning to this example, we would like to treat a continuous source in some generality. The tools needed for such a treatment can be found in Section III. If V_{m1} and V_{m2} represent the wave amplitudes at P_1 and P_2, respectively, for particles originating from the mth source element, then the total registration probability, $W(P_1,P_2)$, for a countable set of emitters is proportional to:

Nucleons: (1)

$$W_N(P_1,P_2) \propto \sum_m \sum_n 3\left\langle |V_{m1}(t)V_{n2}(t) - V_{n1}(t)V_{m2}(t)|^2 \right\rangle$$
$$+ \left\langle |V_{m1}(t)V_{n2}(t) + V_{n1}(t)V_{m2}(t)|^2 \right\rangle$$

Pions: (2)

$$W_\pi(P_1,P_2) \propto \sum_m \sum_n \left\langle |V_{m1}(t)V_{n2}(t) + V_{n1}(t)V_{m2}(t)|^2 \right\rangle$$

Some remarks are in order at this point:

1. The registration probabilities given above are those that enter into the calculation of exclusive (as opposed to inclusive) cross sections. In order to get a better feel for the sort of information contained in either $W_N(P_1,P_2)$ or $W_\pi(P_1,P_2)$, let us consider a specific example. Suppose that the source is composed of three distinct surface elements, each of which emits particles independently of the other two. At any time, the number of particles that may be emitted is zero, one, two, or three. Clearly, since it takes two particles to trigger the detectors in the

experiment we have in mind, zero and one particle emissions are not detectable events. With three particle emissions, however, it is possible to have one particle at each detector (and a third particle somewhere else). But the final state of the source after the emission of three particles is different from the state after a two-particle emission.

In computing $W_N(P_1,P_2)$ and $W_\pi(P_1,P_2)$, we consider only events arising from two particle emissions. This is what is meant by an "exclusive" cross section. On the other hand, the "inclusive" cross section for our two detector experiment would include all processes that lead to a final state with one particle at each detector, regardless of the final state of the source.

2. The second remark concerns the reason behind summing the individual probabilities rather than summing the amplitudes first and then taking the absolute square of the total amplitude. The reason is that the emission of particles by a particular pair of nuclear surface elements leads to a final state distinguishable from the rest.

Let us calculate $W_N(P_1,P_2)$:

$$W_N(P_1,P_2) \propto \Big\langle \sum_m \sum_n \{3|V_{m1}(t)V_{n2}(t)-V_{n1}(t)V_{m2}(t)|^2 + |V_{m1}(t)V_{n2}(t)+V_{n1}(t)V_{m2}(t)|^2\}\Big\rangle$$

The first term arises from those states involving one of the three symmetric spin states, whereas the second term is the spatial part of an overall antisymmetric wave function with an antisymmetric spin part. Observe that particles originating from the same source element can make a finite contribution to $W_N(P_1,P_2)$ so long as the spins of the particles are different.

$W_N(P_1,P_2)$ can be evaluated further:

$$W_N(P_1,P_2) \propto 3\sum_m\sum_n \langle |V_{m1}V_{n2}-V_{n1}V_{m2}|^2\rangle$$

$$+\sum_m\sum_n \langle |V_{m1}V_{n2}+V_{n1}V_{m2}|^2\rangle$$

$$= 3\sum_m\sum_n \Big(\langle |V_{m1}|^2|V_{n2}|^2\rangle + \langle |V_{n1}|^2|V_{m2}|^2\rangle$$

$$- \langle V_{m1}V^*_{m2}V_{n2}V^*_{n1}\rangle - \langle V_{n1}V^*_{m1}V_{m2}V^*_{n2}\rangle\Big)$$

$$+\sum_m\sum_n \Big(\langle |V_{m1}|^2|V_{n2}|^2\rangle + \langle |V_{n1}|^2|V_{m2}|^2\rangle$$

$$+ \langle V_{m1}V^*_{m2}V^*_{n1}V_{n2}\rangle + \langle V_{n1}V^*_{n2}V^*_{m1}V_{m2}\rangle\Big)$$

$$\propto 2\sum_m |V_{m1}|^2 \sum_n |V_{n2}|^2 - \tfrac{1}{2}\langle \sum_m V_{m1}V^*_{m2}\sum_n V^*_{n1}V_{n2}\rangle$$

$$- \tfrac{1}{2}\langle \sum_m V^*_{m1}V_{m2}\sum_n V_{n1}V^*_{n2}\rangle \ .$$

Renaming dummy indices, we have:

$$W_N(P_1,P_2) \propto 2\ \Big[\sum_m |V_{m1}|^2 \sum_n |V_{n2}|^2 - \tfrac{1}{2}\langle (\sum_m V_{m1}V^*_{m2})\ (\sum_n V_{n1}V^*_{n2})^*\rangle\Big]$$

or

$$W_N(P_1,P_2) \propto 2\ \Big[\sum_m |V_{m1}|^2 \sum_n |V_{n2}|^2 - \tfrac{1}{2}\langle |\sum_m V_{m1}V^*_{m2}|^2\rangle\Big] \ .$$

The sums in the first expression on the R.H.S. of the proportionality are independent of time; thus, the time-average brackets have been dropped.

This result resembles the expressions of Section III, where the function of major interest was $J(P_1,P_2) = \sum_m \langle V_{m1}(t)V^*_{m2}(t)\rangle$. As long as $r_{m1}-r_{m2}$ is small compared to the coherence length, we need not fret that

$$\langle \sum_m V_{m1}V^*_{m2}\ \sum_n (V_{n1}V^*_{n2})^*\rangle \neq \sum_m \langle V_{m1}V^*_{m2}\rangle \sum_n \langle (V_{n1}V^*_{n2})^*\rangle :$$

for with $(r_{m1}-r_{m2}) < \ell_{COHERENCE}$, $(V_{m1}(t)\ V^{*}_{m2}(t))$, as written in Section III, loses all time dependence, and hence, there is no longer a time average to take. Since the wave functions of the particles have the same form as the wave amplitudes in Section III, we can write in the continuum limit (just as we did in Section III),

$$W_N(P_1,P_2) \longrightarrow 2\left[\int \frac{I(s)ds}{r_1^2} \int \frac{I(s)ds}{r_2^2} - \frac{1}{2}\left|\int \frac{I(s)}{r_1 r_2} \exp\ i\bar{K}(r_1 - r_2)dS\right|^2\right]$$

which for a uniformly radiating nuclear surface in the shape of circular disk becomes:

$$W_N(P_1,P_2) \propto 2J(P_1,P_1)J(P_2,P_2)\left[1 - \frac{1}{2}\left(\frac{2J_1(V)}{V}\right)^2\right] \quad .$$

The correlation functions, $J(P_1,P_1)$ and $J(P_2,P_2)$, and the argument of the Bessel function, V, are defined precisely as they were in Section III; here, however, $\bar{K}$ can be interpreted as $\bar{p}/\hbar$, where $\bar{p}$ is the average momentum of an outgoing particle.

Since the argument of the Bessel function contains the radius of the source, we have a means of measuring the dimensions of the source: as the detectors, located initially at the same point, are moved apart, the function $[2J_1(V)/V]$ decreases from a maximum value of 1 to 0(V=3.83). Hence, by knowing the detector separation and the average energy of the outgoing particles as well as the distance of the detector from the center of the source disk, the radius, a, of the disk can be, in principle, determined.

We now have solved the problem that we originally set out to solve: the total probability for observing a simultaneous registration of two particles emitted by a uniformly radiating sphere. To see that we have the solution at hand, it is necessary to show that the problem of a uniformly radiating sphere reduces to the one of a uniformly radiating disk. Consider an infinitesimal surface element on the radiating sphere. The contribution of this element to the number of emitted particles in a particular direction is proportional to the projection of the surface onto a plane lying perpendicular to the direction line, D (which is defined by the polar angles (α,β)—see Fig. 4).[6] The projection of a spherical surface onto a plane normal to the direction (α,β) is just a circular disk of radius equal to the radius of the sphere. Hence, the reduction to a disk problem is accomplished.

VI. PROTON COLLISIONS

An interesting application of the ideas presented so far is the mechanism for particle exchange between two colliding protons. The particle that is exchanged can itself emit secondary particles. This exchanged particle will be termed a gluon, although reggeon would be an equally good term. If the pattern of emissions from the exchanged particle is distinguishable from the emission pattern of the colliding protons, then it might be possible to measure the size and shape of the "interaction" region by applying what was learned in the earlier sections. Since opposing theories predict differently shaped reaction regions, correlation measurements of secondary-particle emissions might be able to point to the right theory.

As an illustration of future work that might be done, we will present a multiperipheral picture of the proton-proton collision process (see Figures 5 and 8a,b). Two well-collimated beams of protons, traveling in opposite directions, are allowed to scatter off each other. When any two protons are sufficiently close, there is a possibility that they will interact by exchanging a gluon. The gluon leaves one proton and disappears at the other one. In-between, the exchanged gluon emits a few secondary particles. To make the picture especially simple, we will assume that the path, which the exchanged gluon takes between the protons, is straight and that the emission of a secondary particle at one point along the path is completely uncorrelated with emissions at any other point (We could equally well assume that the path taken by the gluon is curved.). The important point is that after averaging over all curved paths, the mean width of the path is small compared to its length. A third assumption is that there is an equal probability for emission along the path. Finally, the emission pattern of the secondary particles is completely unaffected by any motion of the exchanged gluon. In some sense, then, the exchanged gluon within this picture does not travel from one proton to the other.

When an average over many collisions is taken, the emission problem reduces to that of a uniformly radiating surface, almost rectangular in shape but very narrow.[7] If two detectors are placed parallel to the radiating slit (see Fig. 5), then the total probability for particles to arrive simultaneously at the detectors can be determined. The registration probability for fermion particles is given in Section III):

$$W_N(P_1,P_2) \propto \left[\int \frac{I(s)ds}{r_1^2} \int \frac{I(s)ds}{r_2^2} - \frac{1}{2}\left|\int \frac{I(s)\exp\, i\bar{K}(r_1-r_2)}{r_1 r_2}\, dS\right|^2\right]$$

$$= J(P_1,P_1)J(P_2,P_2)\left[1 - \frac{1}{2}\left|\mu(P_1,P_2)\right|^2\right]$$

$$= J(P_1,P_1)J(P_2,P_2)\left[1 - \frac{1}{2}\left|\frac{\iint I(x',y')\exp\left[-i\bar{K}(px'+qy')dx'dy'\right]}{\iint I(x',y')dx'dy'}\right|^2\right]$$

When the surface radiates uniformly, then $I(x',y')$ can be taken outside the integral, leaving only the integral, $\iint \exp\left[-i\bar{K}(px'+qy')\right] dx'dy'$ to be evaluated. But this integral is the Fraunhofer diffraction result. For a rectangular surface of the dimensions given in Fig. 6,

$$\int \exp -i\bar{K}(px'+qy')dx'dy' = \frac{\sin\bar{K}pa}{\bar{K}pa}\ \frac{\sin\bar{K}qb}{\bar{K}qb}$$

Hence,

$$W_N(P_1,P_2) \propto J(P_1,P_1)J(P_2,P_2)\left[1 - \frac{1}{2}\left(\frac{\sin\bar{K}pa}{\bar{K}pa}\right)\left(\frac{\sin\bar{K}qb}{\bar{K}qb}\right)^2\right]$$

For b sufficiently small such that $\bar{K}qb << 1$,

$$W_N(P_1,P_2) \longrightarrow J(P_1,P_1)J(P_2,P_2)\left[1 - \frac{1}{2}\left(\frac{\sin\bar{K}pa}{\bar{K}pa}\right)^2\right] .$$

These diffraction results can be readily applied to two different experiments. In one experiment, the scattering angle of the protons is measured along with the two-particle registration probabilities. From this information, the orientation of the "radiating slit", the source of the secondary particles, can be inferred. This allows us to select those events at the detectors that correspond to a particular orientation of the slit.

It should be stressed that the region from which the secondary particles emmanate need not have spherical symmetry: we have assumed that the region has a rod-like shape, and, therefore, the configuration of the detectors with respect to a proton trigger must be considered with care. Perhaps the most advantageous orientation of the detectors is the arrangement pictured in Fig. 7, with the detectors placed symmetrically about the perpendicular bisector of the rod and away from the line containing the rod. The radiation pattern for this situation is that of a slit, the projection of the rod onto a plane normal to the perpendicular bisector (which also defines the direction of the detectors). If the registration probability goes as

$$\left[1 - \frac{1}{2}\left(\frac{\sin\bar{K}pa}{\bar{K}pa}\right)^2\right] ;$$

then as the detectors are further separated by moving them along line A (see Fig. 7), the argument of the sine function will vary $\left(\text{Note: } p = \frac{x_{p1}-x_{p2}}{R}\right)$ and variations in the registration probability will be recorded.

Another reason for selecting the arrangement of detectors suggested above lies with the angular distribution of the emitted secondary particles. Though the rod is assumed to emit uniformly—each surface element radiates in the same manner as any other surface piece—this does not rule out the possibility that the distribution of particle emissions is peaked at some angle relative to the axis lying along the length of the rod (the "long axis"). In fact, we can argue from the uncertainty principle that there is a preferred direction of emission. The particle exchanged by two interacting protons is confined to the region defined by the parameters of the rod. Because of the narrowness of the rod, the position of the exchanged particle in the direction normal to the long axis is known very well. By the uncertainty principle, this implies a large uncertainty in the corresponding component of momentum. In general, then, the emitted particles will have more momentum in the direction defined by the perpendicular bisector than along the long axis of the rod; this means that the distribution of secondary particles is peaked about $\theta=90^{\circ}$ (orthogonal to the long axis).

In the second experiment we have in mind, the proton scattering angles are not measured. The data collected by the detectors cannot be assigned to a particular orientation of the radiating rod. Instead, the data represent an averaging over all possible orientations and should roughly correspond to the diffraction pattern for a uniformly radiating disk. A measurement of the radius of the "average" disk provides useful information about the proton-proton interaction region.

SUMMARY

The first sections of this report were concerned with certain correlation functions that arise in the domain of electromagnetic interference phenomena. These functions have deep ties to the principle of superposition, which allows us to find the total disturbance at a given point by simply adding up the individual contributions of the source elements. In Section (I), the correlation function $I(P_1,P_2)=\langle I_1(t)I_2(t)\rangle$, where I_1 and I_2 are the intensities at points P_1 and P_2, respectively, was introduced. The two source-two detector experiment demonstrated that $\langle I_1(t)I_2(t)\rangle$ can have a harmonic spatial dependence even though the relative phases of the sources might be continually changing. The reason for this is that the instantaneous intensity patterns seen by the detectors vary coherently (provided the detectors are sufficiently close to each other).

A second correlation function that entered the discussion was the "time" counterpart of $I(P_1,P_2)$: $I(t,t+\tau) = \langle I_1(t)I_1(t+\tau)\rangle$. This function, as was shown in Section (II), samples the intensity reaching the same detector at two different time points.

In Section (III), the source of the disturbance was no longer restricted to two space points: the definition of source was broadened to include extended, continuous surfaces. The pursuit of this problem led to the introduction of yet a third correlation function: $J(P_1,P_2) = \langle V_1(t)\ V_2^*(t)\rangle$ where V_i is the total wave amplitude at point p_i. That $J(P_1,P_2)$ is not the same as $I(P_1,P_2)$ can be seen by writing

$$I(P_1,P_2) = \langle I_1 I_2\rangle = \langle |V_1(t)|^2 |V_2(t)|^2\rangle$$

$$= \langle |V_1(t)V_2^*(t)|^2\rangle$$

$J(P_1,P_2)$ is an "amplitude" correlation function, whereas $I(P_1,P_2)$ is an "intensity" correlation function. The experiment discussed in Section (I) illustrates the foundations of $I(P_1,P_2)$. A closely related experiment aids in interpreting the meaning of $J(P_1,P_2)$. The experimental set-up for the second experiment is exactly like that for the first; however, instead of taking the product of the intensities at the two detector points, P_1 and P_2, we imagine these two points to be new sources, and we compute the total wave amplitude—originating from P_1 and P_2—at a third, Q, located behind P_1 and P_2. The intensity at Q is then

$$\langle |V_{P_1}(t) + V_{P_2}(t)|^2\rangle$$

which contains terms like

$$\langle V_{P_1}(t)V_{P_2}^*(t)\rangle \ .$$

Such terms represent the correlation between the wave fronts incident at P_1 and P_2.

It was also shown in Section (III) that $\langle V_{P_1}(t)V^*_{P_2}(t)\rangle$ is formally tied to Fraunhofer diffraction theory. This connection is not too surprising in light of the fact that the form $\langle V_{P_1}(t)V^*_{P_2}(t)\rangle$ arises from regarding P_1 and P_2 as secondary sources; the idea that space-points—away from physical sources—are themselves secondary sources is the basis of Huygen's principle and scalar diffraction theory.

In Sections IV and V, an attempt was made to apply the ideas behind the correlation functions to the quantum mechanical problem of neutrons or pions emitted by an excited nucleus. The wave function that was written down to describe the simultaneous registration of two identical particles at two detectors contained terms of the form $V_{m1}(t)V_{n2}(t)$ and $V_{m2}(t)V_{n1}(t)$. The probability for such a process to occur, which is given by the absolute square of the amplitude, involved terms like $V_{m1}(t)V^*_{m2}(t)$, suggesting a link to the function $J(P_1,P_2)$. When the total registration probability for an extended and continuous nuclear surface was computed, it was assumed that, at any given time, only two particles are sufficiently close in space and time to show quantum mechanical interference. Hence, the total probability was a sum of two-body probabilities. Evaluation of the expression for the total probability led to the same "diffraction" integral found in Section III. This allowed us to take over the results of the earlier section and apply them to the nuclear problem.

Finally, in Section VI, further applications of correlation experiments were suggested. In particular, inelastic proton-proton collisions were briefly discussed using a simple multiperipheral type model.

ACKNOWLEDGEMENT

It is a pleasure to thank Professor Richard Blankenbecler for suggesting this problem and for many enlightening and stimulating comments and discussions throughout the course of this work.

REFERENCES

† $\langle\ \rangle$ denotes time average

1. See Born and Wolf, Principles of Optics, 5th Ed., § 10.4.2.

2. Born and Wolf: equations 27 and 30, § 10.3.2.

3. Born and Wolf: p. 511.

4. Kopylov, G. I. and M. I. Podgoretskii, "Correlations of Identical Particles Emitted by Highly Excited Nuclei," Soviet Journal of Nuclear Physics, Vol. 15, No. 2, pp. 219-222.

5. This, however, may or may not be a realistic assumption. See Fowler, G. N. and R. M. Wiener, "Possible Evidence for Coherence of Hadronic Fields from Bose-Einstein Correlation Experiments," Phys. Lett., Vol. 70B, No. 2, p. 201.

6. This is an illustration of Lambert's law. See Born and Wolf, § 4.8.

7. Born and Wolf, § 8.5.1.

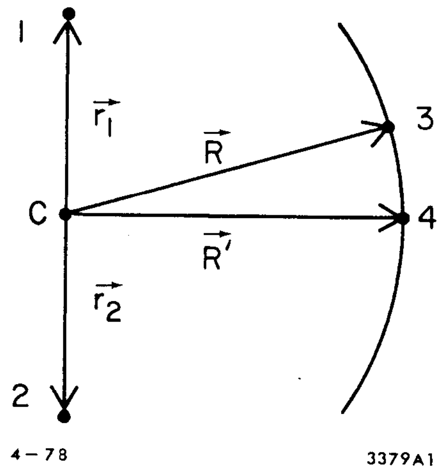

Fig. 1

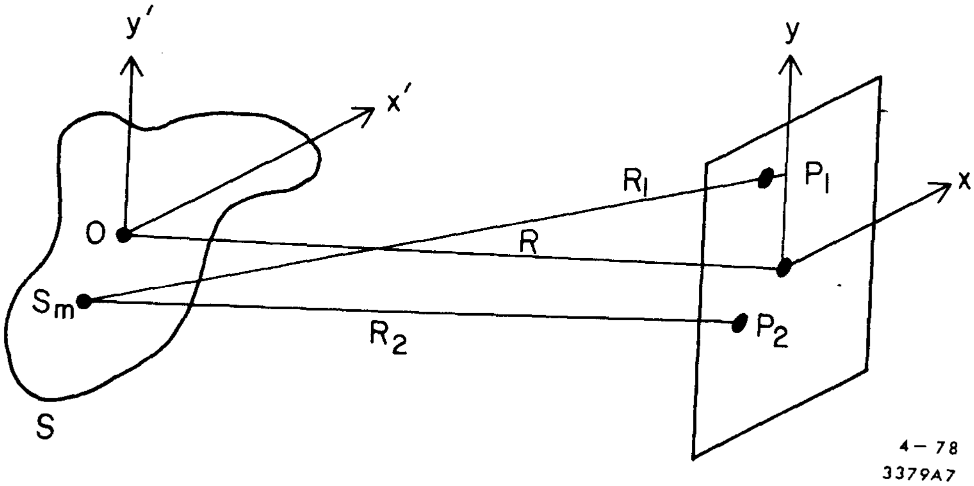

Fig. 2

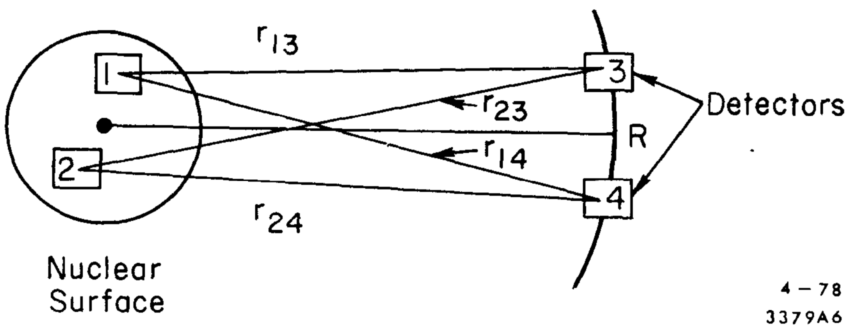

Fig. 3

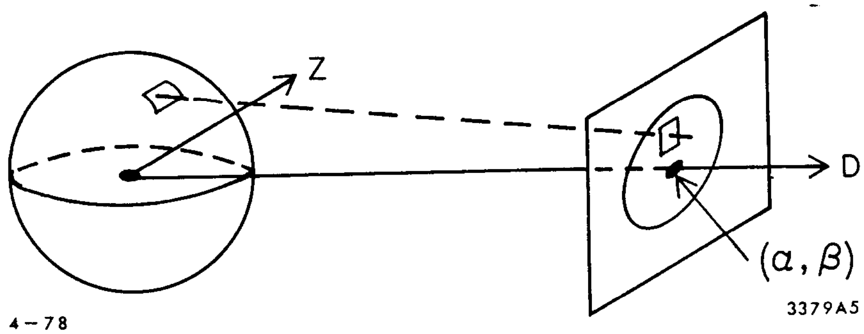

Fig. 4

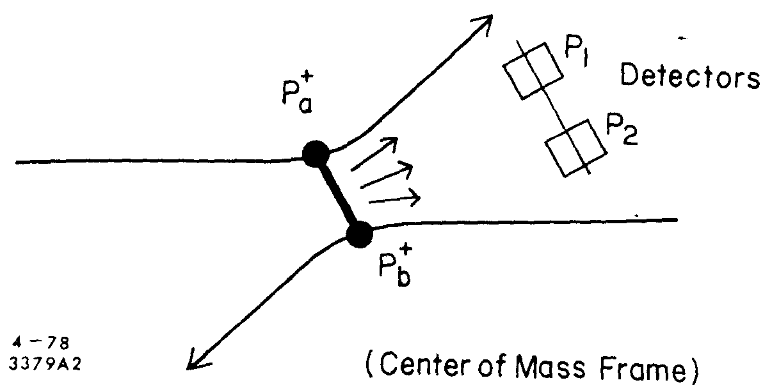

Fig. 5

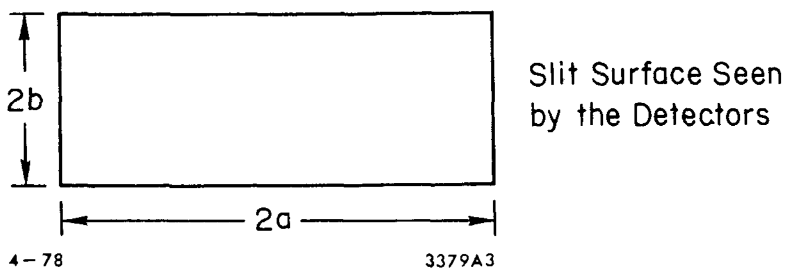

Fig. 6

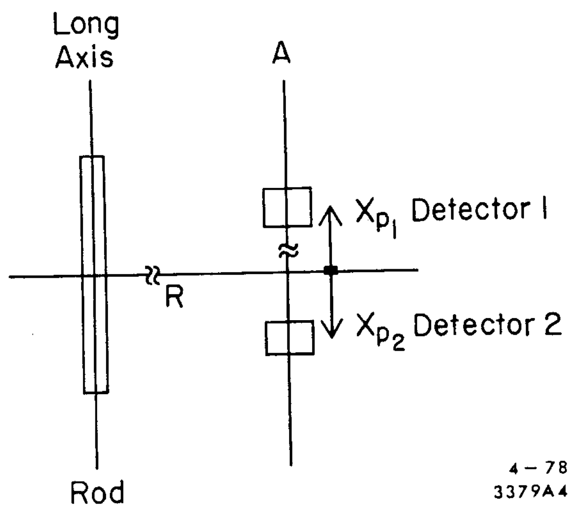

Fig. 7

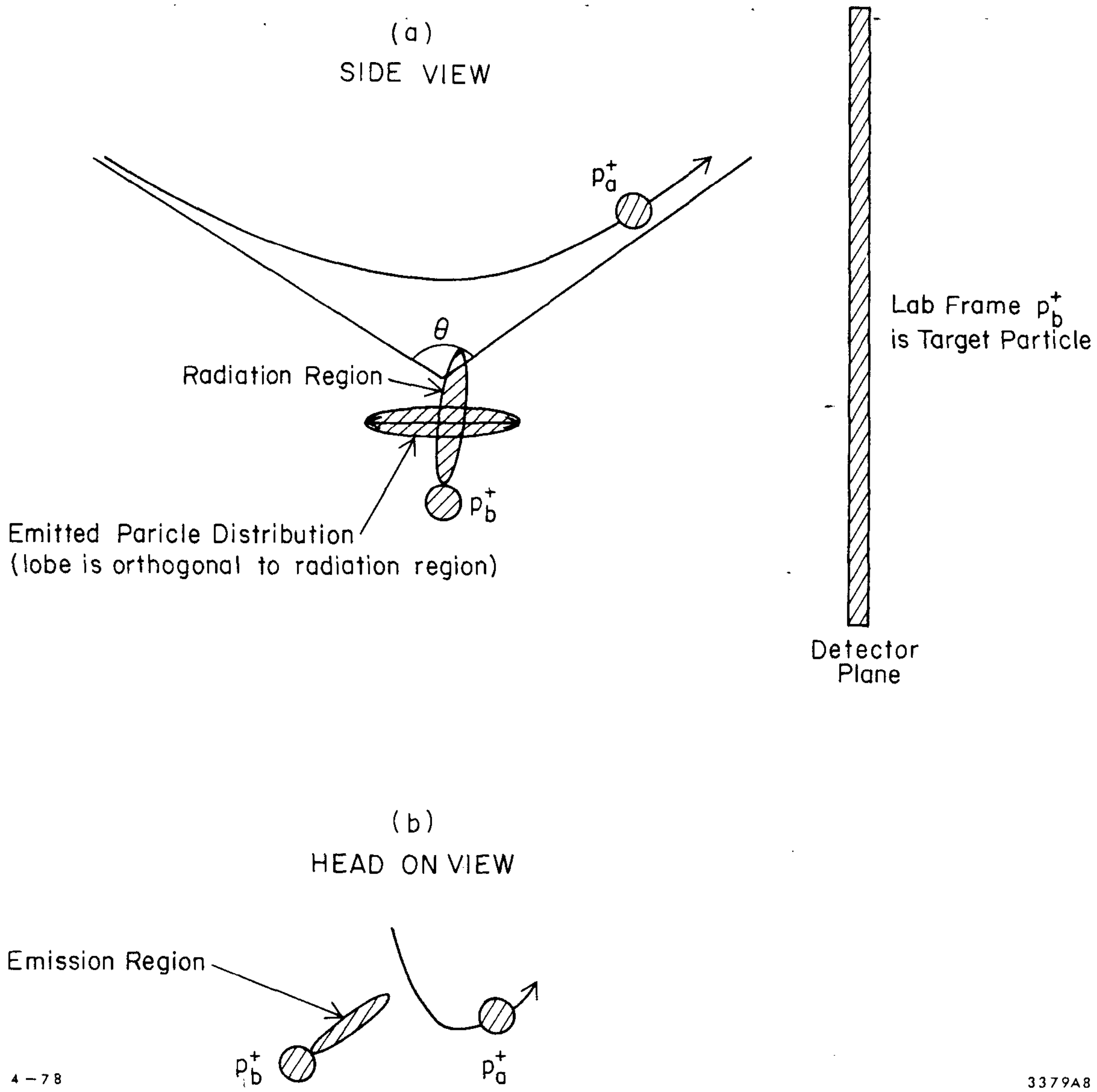
(a)
SIDE VIEW
p_a^+
θ
Lab Frame p_b^+
is Target Particle
Radiation Region
p_b^+
Emitted Paricle Distribution
(lobe is orthogonal to radiation region)
Detector
Plane
(b)
HEAD ON VIEW
Emission Region
p_b^+
p_a^+
4-78
3379A8

Fig. 8